Study of Dispersion in Packed Chromatographic Columns by Pulsed Field Gradient Nuclear Magnetic Resonance

Ulrich Tallarek,[†] Ernst Bayer,[†] and Georges Guiochon*[,‡]

Contribution from the Institut für Organische Chemie, University of Tübingen, D-72076 Tübingen, Germany, Department of Chemistry, University of Tennessee, Knoxville, Tennessee 37996-1600, and Division of Analytical Chemistry, Oak Ridge National Laboratory, Oak Ridge, Tennessee 37831-6120

Received August 4, 1997

Abstract: Pulsed field gradient nuclear magnetic resonance (PFGNMR) allows the direct determination of the average value of the axial and transverse apparent dispersion coefficient in a packed bed over a certain volume of this bed. From these data, the dependence of the local value of the height equivalent to a theoretical plate (HETP) of a chromatographic column on the fluid velocity can be measured accurately. The results are shown to be exactly accounted for by the Giddings equation. The PFGNMR measurements are made over a very short period of time. Hence they give the value of the HETP averaged over a limited volume of packing and a short time. This value is markedly smaller than the one afforded by the classical methods of chromatography and which is derived from the width of the distribution of the residence time of a small sample. The difference is explained by systematic variations of the local mobile-phase velocity across the column. PFGNMR techniques also allow the determination of the tortuosity of the column packing in the absence of flow. Their results confirm that the apparent dispersion experienced by a molecule is a function of the duration of the observation, until the tortuosity of the packing is completely felt. The values obtained agree very well with those derived from classical chromatography determinations.

Introduction

Dispersion in porous media has long been a topic of great importance in engineering. Dispersion of fluids in soil is involved in the detection of oil fields, in the recovery of gas and oil from reservoirs, or in the migration of pollutants in the water table. In chemical engineering, packed beds of catalysts are used in reactors; packed columns are used in various separation methods based on adsorption. The efficiency of one of the most recent of these processes, high performance liquid chromatography (HPLC), depends critically on the extent of axial dispersion taking place during runs. This is especially important in the case of the columns used for the preparative applications of chromatography.[1] An extensive amount of literature exists on this issue. It cannot be reviewed comprehensively here. However, the fundamental work of Ebach and White,[2] Gunn,[3] Gunn and Pryce,[4] and Hiby[5] should be acknowledged. These authors have shown that there is a correlation between the axial and the radial Peclet numbers, which characterize dispersion in these two directions, and the Reynolds number, which characterizes the nature of the flow. Various relationships have been proposed.[2−5] Later, Koch et al.[6] discussed on a theoretical basis the dispersion of solutes in streams percolating through spatially periodic porous media. They demonstrated that, for a square array of cylinders or a cubic array of spheres, the axial dispersion coefficient becomes a quadratic function of the Peclet number (*Pe*) when *Pe* increases indefinitely whereas the transverse dispersion coefficient approaches a constant value. In general, a different behavior is expected and observed for ordered and for randomly packed beds.[7]

In the present work, however, we are concerned only with chromatographic applications and, in this area, such a correlation is known as the plate height equation. The range of Reynolds number within which liquid chromatography is carried out is very low, of the order of 0.001, while all the experimental data acquired for the study of the correlations just mentioned were obtained under experimental conditions for which the Reynolds number is larger than 0.1.[2−5] This explains why the corresponding work has been of little use in chromatography. Important work on the plate height equation has been done by Giddings,[8] van Deemter et al.,[9] Knox,[10] Knox et al.,[11,12] Huber,[13] and Horváth and Lin.[14,15] The conclusions of these different works are still controversial. Despite some attempts at comparing the validity of these equations,[16] we still do not understand sufficiently well the mechanism of dispersion in chromato-

* To whom correspondence should be addressed, at the University of Tennessee.
[†] University of Tübingen.
[‡] University of Tennessee and Oak Ridge National Laboratory.

(1) Guiochon, G.; Farkas, T.; Guan-Sajonz, H.; Koh, J.-H.; Sarker, M.; Stanley, B. J.; Yun, T. *J. Chromatogr. A* **1997**, *762*, 83
(2) Ebach, E. A.; White, R. R. *AIChE J.* **1958**, *4*, 161.
(3) Gunn, D. J. *The Chemical Engineer* **1968**, *46*, CE153.
(4) Gunn, D. J.; Pryce, C. *Trans. Inst. Chem. Eng.* **1969**, *47*, T351.
(5) Hiby, J. W. In *Interaction between Fluids and Particles*; Rottenburg, P. A., Ed.; Institution of Chemical Engineers: London, UK, 1962; p 312.
(6) Koch, D. L.; Cox, R. G.; Brenner, H.; Brady, J. F. *J. Fluid Mech.* **1989**, *200*, 173.
(7) Koch, D. L.; Brady, J. F. *J. Fluid Mech.* **1985**, *154*, 399.
(8) Giddings, J. C. *Dynamics of Chromatography*; M. Dekker: New York, 1965.
(9) Van Deemter, J. J.; Zuiderweg, F. J.; Klinkenberg, A. *Chem. Eng. Sci.* **1956**, *5*, 271.
(10) Knox, J. H. *J. Chromatogr. Sci.* **1977**, *15*, 352.
(11) Knox, J. H.; Saleem, M. *J. Chromatogr. Sci.* **1969**, *7*, 614.
(12) Knox, J. H.; Laird, G. R.; Raven, P. A. *J. Chromatogr.* **1976**, *122*, 129.
(13) Huber, J. F. K. *Ber. Bunsen-Ges. Phys. Chem.* **1973**, *77*, 179.
(14) Horváth, Cs.; Lin, H.-J. *J. Chromatogr.* **1976**, *126*, 401.
(15) Horváth, Cs.; Lin, H.-J. *J. Chromatogr.* **1978**, *149*, 43.

S0002-7863(97)02662-0 CCC: $15.00
Published on Web 02/03/1998

graphic columns to assess the separate contributions of (1) axial dispersion caused by the packing material itself; (2) the mass transfer resistance, which causes an apparent dispersion; (3) the lack of homogeneity of the packed bed; and (4) the extracolumn sources of axial dispersion. A most lucid analysis of the fundamentals of this issue has been done by Giddings.[8,17] He has shown that the magnitude of the problem tends to aggravate with increasing column diameter.[17]

The development of preparative chromatography raises two new issues, ignored in analytical applications. Large diameter columns are operated for industrial applications. Serious difficulties are encountered in achieving homogeneous, stable packed beds.[1,18] Trains of 8−16 large bore columns are used in simulated moving bed separators (SMB) which have, over conventional overloaded elution chromatography, the advantage of operating continuously. This advantage is achieved at the cost of a more sophisticated and expensive instrument and a more complex operation.[19] All the columns of an SMB must be as nearly identical as possible to minimize costly fluctuations of performance during a series of cycles. Thus, the specifications regarding the packing of such columns are severe.[20,21] It is important to investigate the parameters which influence packing homogeneity. The packing media used in chromatography have some interesting properties. The particle size distribution is very narrow compared to that of most other materials in which dispersion is or has been studied. The packed beds obtained have a well-resolved bimodal pore size distribution, with two well resolved modes.[22] The first mode corresponds to the external pores, between particles, through which flows the stream of mobile phase. The second mode corresponds to the internal pores which confer its large specific surface area to the material. Modern commercial packing materials are made of very pure silica gel, containing extremely small amounts of metallic impurities.

It has been shown that the beds of packed chromatographic columns are heterogeneous.[23−27] There is a radial and an axial distribution of the packing density.[1] In slurry-packed columns, the packing density tends to be higher in proximity of the column wall and to decrease toward its center.[23−26] A similar result is obtained with axial compression columns.[27] This has been shown by the results of systematic measurements of the radial distribution of the local velocity of the mobile phase at the column exit. The residence time of compounds injected as an homogeneously distributed band decreases from the wall to the center of the column. Differences of between 3 and 10% between center and wall velocities have been reported, the wider velocity distributions being observed with the columns of lowest efficiency.[23−27] The local efficiency of a column is higher in its center than close to its wall, the ratio of the local values of the height equivalent to a theoretical plate (HETP) along the column axis and close to its wall; depends much on the column efficiency and may easily exceed three for fair or good columns.[23−27] Even though the distribution of the sample concentration over the inlet column cross-sectional area was homogeneous, it was found that this distribution was not homogeneous at the exit. Combined with the observation that the radial velocity distribution is not homogeneous, this suggests that, in a certain volume of the column, the local velocity may have a radial component.[27] These phenomena also explain why peaks recorded with a conventional, on-line detector monitoring the concentration of the bulk eluent tail while the peaks recorded with a local concentration sensor, upon injection of the same sample amount, using the same sampling device, are symmetrical.[27] Finally, it has been shown that packing materials are compressible to a degree (depending on their shape and on the smoothness of their external surface) and that there is a relationship between the packing density distribution and the distribution of mechanical stress during the packing of the column.[28] This implies that friction of the bed along the column wall during column packing should play a role in determining the structure of the packed bed. Local determinations of the axial and transverse dispersion coefficients are necessary to understand better the relationships between the parameters controlling the packing of a chromatographic column, the local distributions of the mobile phase velocity and the local efficiency, and the overall dispersion of the bands obtained, i.e., the performance of the chromatographic column as a separator. Pulsed field gradient nuclear magnetic resonance (PFGNMR) is currently attracting considerable attention as a probe of microscopic properties of porous materials.[29−33] The results of these studies can give volumetrically averaged data. Alternately, combined with NMR imaging techniques, they can provide a contrast mechanism in spatially resolving structural and transport heterogeneities. These measurements are nondestructive and do not involve the introduction of chemical or isotopic tracers. These NMR techniques measure the characteristic response to externally applied magnetic field gradients of the nuclear spins carried by the molecules of the solvent impregnating the material studied (or by particles in suspension in this solvent).[34] Effects arising from motions which are incoherent in nature (e.g., dispersion of molecules in a solvent) can be separated from those originating from coherent displacements (e.g., caused by flow). An independent analysis of the influence of various parameters on these effects and a quantitative comparison of their importance can be carried out easily.[35] Accordingly, local properties of the column are measured without interferences due to the measurement process, as is the case with conventional methods of determination of the column performance.

Furthermore, PFGNMR techniques[33] allow the study of mean square fluid particle displacements as a function of the observation time, the latter being easily adjustable in NMR experiments. In practice, this technique is limited to the measurement of

(16) Magnico, P.; Martin, M. *J. Chromatogr.* **1990**, *517*, 31.
(17) Giddings, J. C. *J. Chromatogr. Sci.* **1962**, *1* (1), 12.
(18) Sarker, M.; Katti, A. M.; Guiochon, G. *J. Chromatogr. A* **1996**, *719*, 275.
(19) Ganetsos, G.; Barker, P. E. *Preparative and Production Scale Chromatography*; Marcel Dekker: New York, 1993.
(20) Broughton, D. B. *Sep. Sci. Technol.* **1985**, *19*, 723.
(21) Stanley, B. J.; Foster, C. R.; Guiochon, G. *J. Chromatogr. A* **1997**, 761, 41.
(22) Guan, H.; Guiochon, G.; Davis, E.; Gulakowski, K.; Smith, D. W. *J. Chromatogr. A* **1997**, *773*, 32.
(23) Baur, J. E.; Kristensen, E. W.; Wightman, R. M. *Anal. Chem.* **1988**, *60*, 2334.
(24) Baur, J. E.; Wightman, R. M. *J. Chromatogr.* **1989**, *482*, 65.
(25) Farkas, T.; Chambers, J. Q.; Guiochon, G. *J. Chromatogr.* **1994**, *679*, 231.
(26) Farkas, T.; Sepaniak, M. J.; Guiochon, G. *J. Chromatogr. A* **1996**, *740*, 169.
(27) Farkas, T.; Sepaniak, M. J.; Guiochon, G. *AIChE J.* **1997**, *43*, 1964.
(28) Train, D. *Trans. Inst. Chem. Eng.* **1957**, *35*, 258.
(29) Proceedings of the 3rd International Meeting on Recent Advances in MRApplications to Porous Media, *Magn. Reson. Imaging* **1996**, *14* (7/8), special issue.
(30) Hallmann, M.; Unger, K. K.; Appel, M.; Fleischer, G.; Kärger, J. *J. Phys. Chem.* **1996**, *100*, 7729.
(31) Rigby, S. P.; Gladden, L. F. *Chem. Eng. Sci.* **1996**, *51*, 2263.
(32) Waggoner, R. A.; Fukushima, E. *Magn. Reson. Imaging* **1996**, *14*, 1085.
(33) Callaghan, P. T. *Principles of Nuclear Magnetic Resonance Microscopy*; Clarendon Press: Oxford, 1993.
(34) Canet, D.; Décorps, M. *Applications of Field Gradients in NMR.* In *Dynamics of Solutions and Fluid Mixtures by NMR*; Delpuech, J.-J., Ed.; Wiley: New York, 1995; Chapter 7.
(35) Callaghan, P. T.; Xia, Y. *J. Magn. Reson.* **1991**, *91*, 326.

dynamic displacements of dispersive origin which are between 10 nm and 100 μm and associated with observation times of a few milliseconds to a few seconds. However, much longer displacements can be encountered in the presence of externally driven convection. This time window is constrained by the maximum available gradient amplitude and by the longitudinal and the transverse relaxation times of the nuclear spins in the environment under study. In closed, isolated systems, for example, the observation time-dependent molecular diffusion coefficient approaches zero eventually because the random molecular displacement is limited by the pore size.[36,37] In connected porous media, by contrast, the bulk diffusion coefficient has a finite asymptotic limit.[38−40] At long observation times, diffusing molecules probe the connectivity of the pore space and the effective or apparent diffusion coefficient is determined by the tortuosity. This macroscopic geometrical parameter relates the diffusivity to many transport properties of fluids confined in porous media, including their permeability or the electrical conductivity of electrolytes.[41] Thus, the determination of the tortuosities and formation factors of porous media by PFGNMR is an attractive, alternative method to electrical conductivity measurements,[42] although the application of these two techniques and the comparison of their results must be made with great caution.[43] For example, the microgeometries of many natural, sedimentary rocks are characterized by mesoscale heterogeneities and broad distributions of pore sizes. In this case, fluid molecules cannot sample representative volumes of the pore space within measurement times which are experimentally accessible in PFGNMR. Strong internal field inhomogeneities caused by the susceptibility contrast between the rock matrix and the water filling the pores may constitute a further source of difficulties.[44,45]

In chromatographic columns, on the other hand, the situation is quite different from the aforementioned one. These columns are packed under high compression stress (dynamic axial compression) or under high viscous compression stress (by pumping a slurry of the packing material under high pressure). The packing materials used are most often based on either monodisperse polymer particles (e.g., cross-linked polystyrene) or porous silica particles exhibiting nearly spherical shape and a narrow particle size distribution. In either case, the connected pore space is less complex than that of sedimentary rocks regarding the scale and range of its heterogeneities. Experimentally achievable measurement times should be sufficient for the asymptotic diffusion coefficient to be monitored by the solvent molecules. By using small size particles, e.g., spherical particles of $\sim$5 μm average diameter, which are readily available, it should be easy to carry out PFGNMR measurements in this asymptotic range. Then, a single measurement could, in principle, give a rough estimate of the tortuosity of the packing. In this way, the PFGNMR method has been used for the determination of tortuosities of porous catalyst support pellets.[46] If it is also possible to catch the initial rapid drop of the dispersion coefficient with increasing observation time (i.e., Δ), important information can be extracted from this decay regarding the ratio of the surface area to the pore volume of the material studied.[38,44] Finally, stationary phases for chromatography are made of high-quality silica with very low amounts of paramagnetic impurities. This allows a large reduction of the magnetic susceptibility contrast across the packed bed, hence of the internal field gradients associated herewith, and results in a better NMR signal-to-noise characteristic.

The applicability of PFGNMR to the determination of axial and transverse apparent dispersion coefficients in packed chromatographic columns as a function of the mobile phase flow velocity was previously illustrated.[47] In this work, we report on the results of measurements carried out for particle Peclet numbers ranging between 0.1 and 140. Columns were packed with spherical particles of porous silica or with monodispersed, strongly cross-linked polystyrene. The experimental data acquired allow a discussion of the velocity dependence of the axial and transverse apparent dispersion coefficients and a comparison of the different models and correlations suggested by van Deemter et al.,[9] Giddings,[8] Knox,[10] Huber,[13] and Horváth and Lin[14,15] to account for this phenomenon. These data also permit the determination of estimates of the values of the tortuosity of the packed bed in the presence and absence of flow through the column. The excellent agreement between these values has important theoretical implications.

Theory

The simultaneous in situ analysis of dispersion and flow velocity in packed columns constitutes a great challenge in liquid chromatography. It has never been solved satisfactorily. PFGNMR affords a most attractive solution.

I. Pulsed Field Gradient Nuclear Magnetic Resonance (PFGNMR). The molecules carrying the nuclear spins move between particles, in the vicinity of impenetrable barriers, the walls of the packing particles. These particles are porous but access to the complex porous microstructure can take place only through a limited number of openings. In the case of externally driven convection, a macroscopic heterogeneity of the molecular displacement originates from the actual radial distribution of the flow velocity over the column cross section. In the measurements of the axial and transverse dispersion coefficients made using the PFGNMR techniques discussed in this work, the flow velocity and the dispersion flux are averaged over the entire cross section of the column and over a length of $\sim$30 mm. In this case, the concept of the so-called averaged propagator, $\bar{P}(\mathbf{R},\Delta)$, has proven to be a very useful formalism in the description of molecular motion reflecting the overall averaging process.[48,49] This averaged propagator describes simply the probability that, independently of its starting position, 0, a molecule undergoes a dynamic displacement $\mathbf{R} = \mathbf{r} - \mathbf{r}_0$ over the observation time Δ. Δ is adjustable. $\bar{P}(\mathbf{R},\Delta)$ is measured in the direction of the applied matched pair of magnetic field gradients selected for a particular PFGNMR experiment, by means of an intertwined radio frequency and gradient pulse scheme which generate a transient NMR signal, called echo. These magnetic field gradients are pulsed for a short time, δ, in the direction parallel or perpendicular to that of the flow velocity. Under their influence, the echo signal will

(36) Wayne, R. C.; Cotts, R. M. *Phys. Rev.* **1966**, *151*, 264.
(37) Wayne, R. C.; Cotts, R. M. *Phys. Rev.* **1967**, *159*, 486.
(38) Latour, L. L.; Mitra, P. P.; Kleinberg, R. L.; Sotak, C. H. *J. Magn. Reson. A* **1993**, *101*, 342.
(39) Sen, P. N.; Schwartz, L. M.; Mitra, P. P.; Halperin, B. I. *Phys. Rev. B* **1994**, *49*, 215.
(40) Dunn, K.-J.; Bergman, D. J. *J. Chem. Phys.* **1995**, *102*, 3041.
(41) Johnson, D. L.; Plona, T. J.; Scala, C.; Pasierb, F.; Kojima, H. *Phys. Rev. Lett.* **1982**, *49*, 1840.
(42) Vinegar, H. J.; Rothwell, W. P. *U.S. Patent No.* 4,719,423, 1988.
(43) Mitra, P. P.; Sen, P. N. *Phys. Rev. B*, **1992**, *45*, 143.
(44) Hürlimann, M. D.; Helmer, K. G.; Latour, L. L.; Sotak, C. H. *J. Magn. Reson. A* **1994**, *111*, 169.
(45) Latour, L. L.; Kleinberg, R. L.; Mitra, P. P.; Sotak, C. H. *J. Magn. Reson. A* **1995**, *112*, 83.
(46) Hollewand M. P.; Gladden, L. F. *Chem. Eng. Sci.* **1995**, *50*, 309.
(47) Tallarek, U.; Albert, K.; Bayer, E.; Guiochon, G. *AIChE J.* **1996**, *42*, 3041.
(48) Kärger, J.; Heink, W. *J. Magn. Reson.* **1983**, *51*, 1.
(49) Kärger, J.; Pfeifer, H.; Heink, W. *Adv. Magn. Reson.* **1988**, *12*, 1.

capture the essential features arising from the combination of diffusivity, convection driven dispersion (see next section), and the net effects of flow over time Δ, as displayed by the associated axial or transverse averaged propagator. In practice, advantage is taken of the direct Fourier relationship between the averaged propagator and the normalized echo amplitude, $\mathbf{R}(\mathbf{g},\delta,\Delta)$, in an ideal PFGNMR experiment (i.e., one for which $\delta \ll \Delta$):[50,51]

$$R(\mathbf{g},\delta,\Delta) = \frac{S(\mathbf{g},\delta,\Delta)}{S(0,\delta,\Delta)} = \int \bar{P}(\mathbf{R},\Delta)\, \exp(i\, \gamma\delta\, \mathbf{g}\cdot\mathbf{R})\, d\mathbf{R} \quad (1)$$

In this equation, $\mathbf{g}$ is the vector (i.e., the amplitude and direction) of the pulsed magnetic field gradients, γ is the gyromagnetic ratio of the nucleus considered, and $S(0,\delta,\Delta)$ and $S(\mathbf{g},\delta,\Delta)$ are the echo signals acquired in the absence and presence of the externally applied field gradients, respectively.

The axial and transverse apparent dispersion coefficients are measures of the average long-range molecular displacements in the porous packing, for which the associated averaged propagator can be described by a Gaussian function. Then, $R(\mathbf{g},\delta,\Delta)$ is also Gaussian and incorporates, in the general case, the effect of externally driven flow superimposed on the dispersive displacements. Thus, it takes the form of an oscillating function of $\mathbf{g}$, modulated by a Gaussian decay:

$$R(\mathbf{k},\Delta) = \frac{S(\mathbf{k},\Delta)}{S(0,\Delta)} = \exp\left[i\mathbf{k}\cdot\mathbf{u}\Delta - k^2 D_{ap}\left(\Delta - \frac{\delta}{3}\right)\right] \quad (2)$$

where $\mathbf{u}$ is the cross-sectional averaged mobile phase velocity and D_{ap} is the apparent axial or transverse dispersion coefficient, depending on the orientation of the magnetic field gradient with respect to the flow velocity, $\mathbf{k} = \gamma\delta\mathbf{g}$, and $k = \gamma\delta g$ is the amplitude of $\mathbf{k}$.

Equation 2 demonstrates the power of the PFGNMR method in distinguishing coherent from incoherent motions. The combined effect of dispersion and convective migration of the molecules studied on the echo signal is a phase shift due only to flow and a net attenuation of the signal intensity, caused only by dispersion. The separation of these two contributions is straightforward and leads to the separate determinations of $\mathbf{u}$ and D_{ap}, respectively. In this work we are only interested in the determination of the apparent dispersion coefficient. We derived it from the initial attenuation of the echo signal observed in the range of small values of $\mathbf{k}$,[45] with $\mathbf{k}(D_{ap}\Delta)^{1/2} \ll 1$, corresponding to long-range displacements in the Fourier sense of eq 1.[52,53]

II. Dispersion in Chromatographic Columns. In chromatography, we define the height equivalent to a theoretical plate (HETP, H) as the slope of the dependence of the variance of a band on the migration distance.[8] As a first approximation, assuming the column to be homogeneous and the mobile phase noncompressible, this slope, hence the HETP, is constant along the column. A similar definition applies to the band broadening in the axial direction, i.e., parallel to the flow velocity, and in the transverse direction. The reduced plate heights ($h = H/d_p$, d_p, particle size) along the column axis (h_a) and in the perpendicular direction (h_t) are given by

$$h_a = \frac{H_a}{d_p} = \frac{1}{d_p}\frac{\partial \sigma_a^{\,2}}{\partial z} \quad (3a)$$

$$h_t = \frac{H_t}{d_p} = \frac{1}{d_p}\frac{\partial \sigma_t^{\,2}}{\partial z} \quad (3b)$$

The band broadening in the axial direction controls the resolution between the peaks of the different components of the sample and is of paramount importance in all applications of chromatography. The band broadening in the transverse direction controls radial homogeneity of the band and relaxes the radial concentration gradients caused by nonuniform distributions of the local permeability, porosity, and packing density.

Since the plate height is constant along the column, it can be derived simply from experimental determinations of the band spreading at the column outlet. Conventional methods in chromatography involve the injection of narrow pulses and the determination of the width of the signals recorded at the column exit, using an on-line detector. This method has the advantage of supplying a figure of merit of the column studied, its HETP, which is directly related to the purpose of chromatography, separating substances. However, this result is difficult to relate to the properties of the column bed as it is sensitive to a number of error sources. First, the band injected is not infinitely narrow and the detector has a finite volume and a finite response time. These extracolumn sources of band broadening cause a positive bias of the measurements.[54] Second, if the column is not homogeneous, the average values obtained for h_a and h_r are difficult to relate to any local property of the column.

Conventional chromatographic methods give the distribution of the residence times of the molecules contained in the injected band. Systematic variations of the local velocity across the column could cause the same amount of band broadening as an irregular packing or the use of a poor packing material. The NMR techniques used in this work afford local values of the band dispersion, hence its HETP, averaged over a certain volume of column and a short period of time. They are insensitive to extracolumn effects since the local dispersion of mobile phase components is directly measured. Thus, they provide an average of the local dispersion coefficients. Because the values of the HETP obtained are derived from dispersion coefficients averaged over short period of times, they are independent of the local distribution of the mobile phase velocities. Thus, they afford a powerful tool for the study of local column properties since they allow direct access to their distribution.

a. The Plate Height Equation. Experiments show that the column HETP is a function of the mobile phase velocity, u. The equation

$$h = f(u) \quad (4)$$

is the plate height equation. Many publications, too numerous to be all acknowledged here, have discussed this relationship.[8,47,55,56] We present briefly the most important of the relationships derived and compare their properties. These equations have in common the use of the reduced velocity or particle Peclet number to characterize the mobile phase velocity

$$\nu = \frac{u d_p}{D_m} \quad (5)$$

where d_p is the average particle diameter and D_m the molecular diffusivity of the solute used for the determinations. The use

(50) Stejskal, E. O.; Tanner, J. E. *J. Chem. Phys.* **1965**, *42*, 288.
(51) Stejskal, E. O. *J. Chem. Phys.* **1965**, *43*, 3597.
(52) Seymour, J. D., Callaghan, P. T. *J. Magn. Reson. A* **1996**, *122*, 90.
(53) Mitra, P. P.; Sen, P. N.; Schwartz, L. M.; Le Doussal, P. *Phys. Rev. Lett.* **1992**, *68*, 3555.
(54) Sternberg, J. C. *Advances in Chromatography*; Marcel Dekker: New York, **1966**; Vol. 2, 205.
(55) Poole, C. F.; Poole, S. K. *Chromatography Today*, 2nd ed.; Elsevier: Amsterdam: The Netherlands, 1993.

of this parameter has the advantage of eliminating the obvious influence of these two parameters, particle size of the packing and molecular diffusivity of the solute, on the dependence of the HETP on the mobile phase velocity.

b. The Giddings Equation. Apparent axial dispersion in chromatographic columns is mainly due to a combination of three effects. The first one or axial diffusion is the spreading due to molecular diffusion, in the direction of the concentration gradient, which goes from the band center to its two ends, where the concentration becomes asymptotically nil. The second one or eddy diffusion is due to the local fluctuations of the mobile phase velocity in a packed column in which the anastomosis of the channels causes important and rapid changes in the velocity. The third one or mass-transfer resistance is caused by the need of a finite time for molecules to diffuse across the porous particles of the packing material, get adsorbed and desorbed, and leave the particle for the mobile phase stream.

Giddings[8] did a detailed analysis of these different effects, including that of stream splitting (see later), based on the use of the random-walk model. This analysis led him to suggest the following plate height equation

$$h_a = \frac{2\gamma}{\nu} + \frac{2\lambda}{1 + \omega\nu^{-x}} + C\nu \qquad (6)$$

where γ is the tortuosity coefficient (unfortunately, defined in chromatography as the reverse of its conventional definition in the material sciences), λ and ω are geometrical parameters which are also weak functions of the retention factor, and x is a constant which, in Giddings equation is equal to 1. The random-walk model used assumes a linear dependence of the convective mass transfer rate on the linear velocity of the fluid. The third term of eq 6 can account only for the mass-transfer processes taking place inside the particles. These assumptions may render the model invalid at high flow velocities, although it is unclear in which range it may falter.

Obviously, an analysis similar to the one performed by Giddings leads to the following expression for the transverse plate height

$$h_t = \frac{2\gamma}{\nu} + D \qquad (7)$$

where D is a coefficient which accounts for the contribution of eddy dispersion to transverse dispersion. It has been related to the phenomenon known as *stream* splitting in fluid mechanics (see later).

c. The Generalized Giddings Equation. While the first and third term of eq 6 are relatively independent of the packing density and of the bed structure, except for the relationship between u and the packing density through the local permeability, this is not true for the second term. Eddy diffusion results directly from the fluctuations of the local mobile phase velocity across the whole column. These fluctuations exist at different scales in the column. For example, at the scale of a particle diameter, they arise from the dependence of the velocity in a channel on the distance from the nearest solid surface; at the scale of a few particle diameters, they arise from the anastomosis of the channels between particles; at the scale of many particles diameters, they are caused by fluctuations in the packing density. It follows that eq 6 should be rewritten as

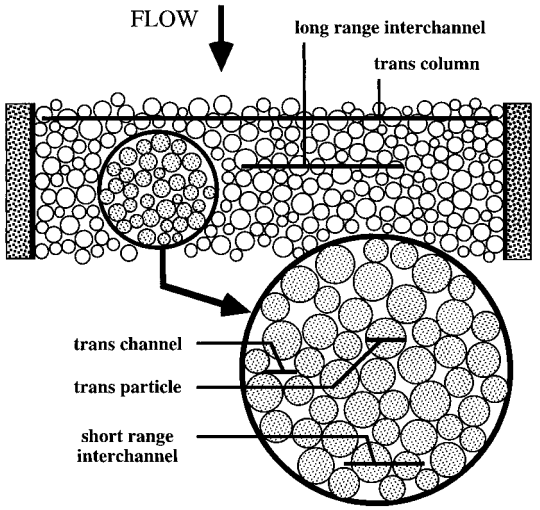

Figure 1. Definitions, locations, and scales of the different classes of velocity fluctuations contributing to eddy dispersion.

$$h = \frac{2\gamma}{\nu} + \sum_i \frac{2\lambda_i}{1 + \omega_i\nu^{-1}} + C\nu \qquad (8)$$

Rather than trying to estimate the average contribution of all these velocity inequalities, Giddings[8] has divided them into five different groups, illustrated in Figure 1. Four of these contributions originate in the stream of mobile phase percolating through the column bed. The *transchannel* contribution arises from the radial distribution of the velocities inside each individual channel. It is somewhat similar to the one arising from the Hagen−Poiseuille flow profile in a cylindrical tube, but channels in a packed column have a much more complicated structure and flow velocity distribution. The *short-range interchannel* contribution is caused by small groups of particles being more closely packed than average and separated by more loosely packed regions. The *long-range interchannel* contribution is a consequence of the fluctuations of the density of these loose agglomerates. Finally, the *transcolumn* contribution originates from systematic variations of the packing density across the entire column, in the transverse and axial directions. So, the sum in eq 8 is (somewhat arbitrarily) limited to four terms. Under these conditions, the values of the parameters estimated by Giddings[8] on the basis of appropriate models for these transchannel short-range, long-range, and transcolumn contributions are 0.5, 0.5, 0.1, and 0.04 m^2 (m, ratio of column to particle diameters) for $2\lambda_i$ and 100, 2.0, 0.1, and 40 for ω_i, respectively. This model is a compromise between completeness (which would require a statistical analysis of the channels distribution and the derivation of the relationship between this distribution, the mobile phase velocity, and the dispersion) and tractability (besides the extreme complexity of the results of the statistical analysis, there would be extreme difficulties in determining independently the value of the numerical parameters so introduced). It has been tested carefully only once,[16] until recently.[47,57]

Giddings[8] identified a fifth contribution, the *transparticle* contribution. However, there is no significant contribution of convection in the migration of the molecules through a particle. Thus, this contribution identifies with that of the intraparticle mass-transfer resistances, accounted for by the third term in eq 8.

(56) Weber S. G.; Carr, P. W. In *High Performance Liquid Chromatography*; Brown, P. R., Hartwick, R. A., Eds.; Wiley: New York, 1989; Chapter 1.

(57) Baumeister, E.; Klose, U.; Albert, K.; Bayer, E.; Guiochon, G. *J. Chromatogr. A* **1995**, *694*, 321.

(58) Lapidus, L.; Amundson, N. R., *J. Phys. Chem.* **1952**, *56*, 984.

d. Alternative Plate Height Equations. 1. The van Deemter Equation. The first plate height equation ever suggested was due to van Deemter et al.[9]

$$h = a + \frac{b}{\nu} + c\nu \tag{9}$$

This simple equation has been derived from an analysis of the analytical solution derived by Lapidus and Amundson[58] to the general rate model of chromatography. Chromatography is a quite impractical separation method when the mass-transfer kinetics across the column is slow. van Deemter et al. have shown that, if the mass transfer kinetics is fast, the concentration profile obtained by Lapidus and Amundson becomes equivalent to a Gaussian distribution. They related the variance of this Gaussian, hence the HETP, to the parameters of the analytical solution of Lapidus and Amundson.[9] The first term of eq 9 accounts for molecular diffusion, the second for eddy diffusion and the third for mass-transfer resistances. It has been reported that this equation fits well the experimental data acquired in a narrow range of velocities.[59] However, since the coefficient of the eddy diffusion term is constant, it cannot account for data acquired in a wide range of velocities.

2. The Knox Equation. Knox and Saleem[11] have derived the most popular plate height equation in an attempt to find a simple equivalent to the generalized Giddings equation (eq 8). Considering a number of sets of experimental data, they found that the following equation was a good empirical correlation

$$h_a = \frac{b}{\nu} + a\nu^n + c\nu \tag{10}$$

with a, b, c, and n numerical coefficients, functions of the compound studied and particularly of its retention factor, of the packing material used, and of the homogeneity of the column bed prepared. The first term accounts for axial diffusion, the second for a combination of eddy and axial dispersion, and the last for the mass-transfer kinetics. The value of n is between 0.2 and 0.35 and is most often taken as $^1/_3$ in the chromatographic literature.[10,55,60−62] Note that the van Deemter equation[9] corresponds to the case in which $n = 0$.

3. The Huber and Horváth Equations. Two other plate height equations have been proposed. Huber[13] used a correlation derived through a dimensional analysis of the data collected by Hiby[5] to calculate the dispersion term arising from the flow heterogeneity. He derived an equation which is identical with eq 6 but with $n = 0.5$. However, the constants ω and C in eq 6 have different physical meaning in the Huber and the Giddings equation. This equation is not based on a physical model but on an empirical correlation of questionable validity.[63] It has not been studied in detail nor compared to experimental data.

Horvàth and Lin[14,15] have assumed that axial dispersion takes place only in the mobile phase which is outside the stagnant film surrounding each particle of the packing. The thickness of this film, δ, decreases with increasing fluid velocity. To estimate δ, these authors assumed that it is equal to the thickness of the Nernst diffusion layer, D_m/k_f, with k_f rate coefficient of mass transfer. Using experimental results from Pfeffer and Happel[64] who showed that the Sherwood number, $Sh = k_f d_p/D_m$, increases in proportion to the power $^1/_3$ of the reduced velocity, they obtained

$$\delta = \frac{d_p}{\omega \nu^{1/3}} \tag{11}$$

This value of the stagnant film thickness allowed the derivation of the plate height equation, eq 6 with $n = {}^1/_3$. A complex investigation of the dependence of experimental values of the column plate height on the different physical parameters included in the explicit expressions of λ, ω, b, and c in eq 6 led Horvàth and Lin[15] to show good agreement with this equation. Later, Arnold et al.[65] showed that the relationship derived by Pfeffer and Happel[56] between the Sherwood number and the reduced velocity is valid only at high values of ν, above ∼50. At low values of ν, they suggested that the Sherwood number would become constant and that the Horváth and Lin equation would reduce under such conditions to the van Deemter equation (eq 9). However, Nelson and Galloway[66] have shown that, although the Sherwood number becomes constant at low velocities for a single particle, the situation is different and more complex for a densely packed bed. In this case, the Sherwood number becomes proportional to the Reynolds number. If this dependence is substituted in the thickness of the Nernst layer (eq 11), we obtain eq 6, with $n = 1$, i.e., which is identical to the Giddings equation. Note, however, that the meaning of the numerical constants of eq 6 is entirely different in the two models.

e. Comparison of Plate Height Equations with Experimental Data. Equation 10 has been widely used in the literature. It explains reasonably well most experimental data.[10−12,60−62,67] This is in part due to the narrow range of values of the reduced velocity within which most of these data have been acquired. It is not easy to operate at high reduced velocities columns packed with the fine particle materials currently available.[62] Extremely high inlet pressures would be required, causing major instrumental problems.[68] On the other hand, from a chromatographic point of view at least, it is of little interest to operate them at values of ν below 1. So, in most cases, experimental correlations have been studied in the range of ν between 1 and 20 to 40.[55,59−62,68] This is barely sufficient for an accurate estimate of a. In most cases, the estimates obtained for b and/or c are poorly precise. This situation explains why the Knox equation (eq 10) has been much more widely used than the more complex Giddings equation (eq 6 with $n = 1$), let alone the generalized Giddings equation (eq 8). The determination of accurate values of the 10 parameters in eq 8 from experimental data acquired in this narrow range of ν would be practically impossible. Even the determination of the four parameters in eq 6 is difficult.

There have been few experimental studies of axial dispersion. Because chromatographic analysis should be carried out in the range of velocities within which the HETP increases with increasing velocity, so that column efficiency can be traded for shorter analysis time, chromatographers have paid little attention to the lower range of velocities, in which axial dispersion controls band spreading. A number of experimental results have

(59) Katz, E.; Ogan, K. L.; Scott, R. P. W. *J. Chromatogr.* **1983**, *270*, 51.
(60) Unger, K. K.; Messer, W.; Krebs, K. F. *J. Chromatogr.* **1978**, *149*, 1.
(61) Kirkland, J. J. *J. Chromatogr. Sci.* **1972**, *10*, 593.
(62) Colin, H.; Diez-Masa, J. C.; Czaychowska, T.: Miedziak, I.; Guiochon, G. *J. Chromatogr.* **1978**, *167*, 41.
(63) Deelder, R. S. *J. Chromatogr.* **1970**, *47*, 307.
(64) Pfeffer, R.; Happel, J. *AIChE J.* **1964**, *10*, 605.
(65) Arnold, F. H.; Blanch, H. W.; Wilke, C. R. *J. Chromatogr.* **1985**, *330*, 159.
(66) Nelson, P. A.; Galloway, T. R. *Chem. Eng. Sci.* **1975**, *30*, 1.
(67) Horne, D. S.; Knox, J. H.; McLaren, L. *Sep. Sci. Technol.* **1966**, *1*, 531.
(68) Scott, R. P. W.; Kucera, P. *J. Chromatogr.* **1979**, *169*, 51.
(69) Giddings, J. C.; Robison, R. A. *Anal. Chem.* **1962**, *34*, 885.

been acquired on packed capillary columns in gas chromatography,[69−72] with values of the column to particle diameter ratio in the order of 4. These columns have a high permeability, demonstrating a lower packing density than average,[71] and a low value of the reduced HETP, often close to 1. These results show that the contribution of transchannel dispersion to overall axial dispersion is moderate, in agreement with a value of ω larger than 10 suggested by the data in ref 69.

Magnico and Martin[16] have packed a wide 16.6 × 2.4 cm column with coarse but homogeneous 200 to 220 μm solid glass beads. The column was packed with unusually great care to achieve a packed bed as homogeneous as possible. They derived the column efficiency from the profiles of breakthrough curves, which were close to error functions, as expected in linear chromatography. The data obtained in a wide range of reduced flow velocities, from 0.5 to 300, were in excellent agreement with the Giddings equation (eq 6). Parameter identification gave best estimates of 1.06 and 10.3 for 2λ and ω, respectively. Comparing these values to the estimates of these parameters made by Giddings for the four different contributions, the author concluded that their data showed that only transchannel and short-range interchannel dispersion (with values of $2\lambda = 0.5$ and 0.5 and $\omega = 100$ and 2.0, respectively) account for dispersion in their columns.[16] Conversely, long-range interchannel and transcolumn dispersion (with values of $2\ \lambda = 0.1$ and 522, $\omega = 0.1$ and 40, and $m = 114$, respectively) should account for the higher dispersion observed in conventional columns.

Recently, Tallarek et al.[47] have measured the axial and transverse dispersion coefficients in a conventional chromatographic column packed with porous silica gel for reduced velocities between 0.08 and 40. Using PFGNMR, they were able to make measurements of the dispersion coefficients of the components of the mobile phase, which eliminates the possible contributions of the injection and the detection system, which can be significant and are always difficult to correct properly.[54] They observed results which were in agreement with the Giddings equation (eq 6). The best estimates of the coefficients of this equation were $\gamma = 0.52$, $\lambda = 3.51$, $\omega = 35.3$, and $C = 0.015$. These values are somewhat different from those derived by Magnico and Martin[16] ($\gamma = 0.6$, $\lambda = 0.53$, $\omega = 10.3$, and $C = 0$). The first one suggests a slightly lower tortuosity, not a surprising result when comparing beds of glass beads and of porous silica gel. (Note also that there are fewer data points at flow velocities lower than the optimum for minimum H than at higher ones, suggesting a higher error for the estimates of γ than for those of ω.) The values of the parameter C were also expected, since the particles used were porous[47] and solid,[16] respectively. The values of the two parameters of the eddy dispersion term are quite different. The value of λ found by Magnico and Martin[16] is in agreement with the value calculated by Giddings for transchannel and short-range interchannel dispersion. The value measured by Tallarek et al.[47] is seven times larger. It could be explained by a transcolumn contribution which was negligible in the earlier experiments[16] but significant with porous particles. Still considerable uncertainty exists regarding the interpretation of these parameters, even if the validity of the Giddings equation seems to be finally established.

f. Transverse Dispersion. If we consider the distribution of streamlets in a packed bed, we observe that they split when they hit a particle, which is a rather frequent event. This produces smaller streamlets of unequal sizes which move around the particle, between it and its neighbor. In the process they encounter other streamlets and merge with them. Thus, the migration of the fluid phase along a packed column is accompanied by the constant shearing and merger of streamlets. This process is involved in the eddy dispersion contribution to axial dispersion. It is also the essential source of radial dispersion. In this case, it is known as stream splitting. Because streamlets are approximately 10 times smaller than the particles between which they flow, transverse dispersion causes the rapid local homogenization of the stream composition. In the absence of significant radial convection, however, this homogenization is extremely slow at the scale of the column diameter.

Using a random-walk model, Saffman[73,74] has investigated this problem in the case of a cylindrical, isotropic bed of solid particles. Two solutions were derived, depending on whether molecular diffusion contributes significantly or not to radial dispersion. In chromatographic columns, the reduced velocity is rarely below 2 and convective dispersion is the controlling phenomenon. From the transverse dispersion coefficient derived by Saffman,[73] the following value of the reduced radial HETP can be calculated

$$h_r = \frac{2\gamma}{\nu} + D \tag{12}$$

On theoretical grounds, Saffman estimated the value of D to be approximately 0.375. The simple random-walk model of Giddings[8] was used by Horne et al.[67] to calculate an estimate of the reduced radial HETP. The value obtained ($D = 1/a\pi^2$, a, constant between 0 and 1, d_p/π, elementary transverse step in the model) is constant and between 0 and 0.2.

Knox et al.[12] recorded simultaneously elution chromatograms at different points of the exit of a column, upon local injection of a sample. From the radial spreading of the band they derived a value of the coefficient D in eq 12 which is constant for reduced velocities between 16 and 250 and equal to 0.060. Using a similar method, Eon[75] found a value of $D = 0.075$ for measurements of the transverse dispersion carried out in the range of reduced velocities between 0.6 and 1000. From on-column measurements carried out by PFGNMR in a much narrower range of reduced velocities, 0.2 to 4, Baumeister et al.[57] derived a value of $D = 0.201$. The column was packed by sedimentation and this high result can probably be explained by a low packing density. Finally, Tallarek et al.[47] obtained values of D equal to 0.14 for acetone on a column packed with 30 μm particle silica and values of 0.27, and 0.31 for acetonitrile and methanol, respectively, on a column packed with 5 μm particles of a different brand of silica. These results seem to suggest a trend, the value of D increasing with decreasing particle size. They are far too limited to allow any final conclusion, however.

Experimental Section

I. NMR Measurements. a. Instrument. PFGNMR measurements were carried out at 19 ±0.5 °C on a Bruker (Karlsruhe, Germany) MSL 200 based spectrometer equipped with an Oxford 4.7 T, 89 mm bore superconducting magnet. By using one of its endfittings, the column was fixed to a home-built sample holder that kept it tightly fixed during the measurements and centered in the rf insert and gradient system. The experimental setup is outlined in Figure 2. The column axis is parallel to the main (static) magnetic field, $\mathbf{B}_o$. The proton

(70) Giddings, J. C. *Anal. Chem.* **1963**, *35*, 1338.
(71) Halasz, I.; Heine, E. *Nature* **1962**, *194*, 971.
(72) Sternberg, J. C.; Poulson, R. E. *Anal. Chem.* **1964**, *36*, 1492.
(73) Saffman, P. G. *J. Fluid Mech.* **1959**, *6*, 321.
(74) Saffman, P. G. *J. Fluid Mech.* **1960**, *7*, 194.
(75) Eon, C. H. *J. Chromatogr.* **1978**, *149*, 29.

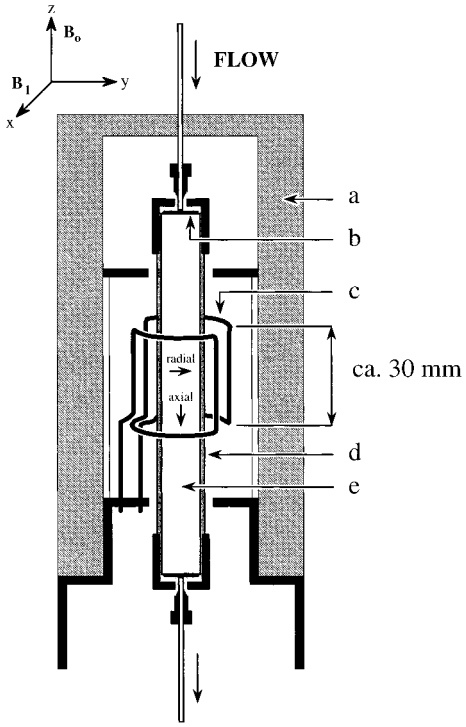

Figure 2. Configuration of the NMR instrument for PFGNMR measurements in chromatographic columns: (a) 40 mm i.d. gradient system, capable of providing pulsed magnetic field gradients in the *x*, *y*, or *z* direction, i.e., parallel or perpendicular to the column axis; (b) biocompatible frit (UHMWPE or PEEK); (c) 15 mm i.d. rf coil; (d) 4.4 mm i.d. PEEK column; and (e) porous packing.

resonance was tuned to 200.13 MHz. Field gradient pulses up to 50 G/cm were applied to the sample, using a Bruker B-GA WB1 self-shielding gradient system of 40 mm i.d. In the axial direction (i.e., parallel to $\mathbf{B}_o$), it provides linear field gradients over approximately 38 mm. A 15 mm i.d. birdcage resonator was used for the rf pulses. In the absence of externally applied field gradients, the line width of the water resonance signal in the porous packing was around 45 Hz.

b. Procedures. In the course of a single measurement for the determination of the axial or transverse dispersion coefficient of water at a given flow rate, the gradient amplitude, **g**, was incremented typically in 16 steps, while δ and Δ were kept constant. Up to 120 phase-cycled echoes were accumulated at each gradient step. The coefficient of apparent dispersion was then calculated from the initial attenuation of the absolute echo intensity. For our experiments, we employed the pulsed field gradient spin−echo sequence (PFGSE),[50] the stimulated echo version (PFGSTE)[76] to realize observation times, Δ up to 1.85 s, and the alternating pulsed gradient stimulated echo technique (APGSTE)[38,77] to allow for additional conclusions about the magnetic susceptibility effects in some porous media packings studied by PFGNMR at 4.7 T.

As shown in Figure 2, the axial and transverse dispersion coefficients measured are averaged values of the local coefficients over the column crosssection and a column length of approximately 30 mm. This volume is located in the middle of the column, eliminating the possible end effects reported elsewhere.[12,23−28,78]

By choosing the spacial direction of the pulsed magnetic field gradient, **g**, either parallel or perpendicular to the column axis, hence of the average direction of the flow velocity, it is possible to measure independently and accurately the axial and the transverse dispersion coefficients, respectively (see eq 2). It is also possible to measure the local flow velocity. The principle of these measurements is illustrated in Figure 3, parts a and b. These two parts show the water resonance signals recorded for the successive 16 steps made in increasing the field gradient, at constant values of δ and Δ. The effects of the dispersion and the flow velocity on the signal increase with increasing **g**. These signals are derived by Fourier transform of the second half of the echo signal acquired. The absolute signal amplitude decays following a Gaussian law. The dispersion coefficient is derived from the variance of this law.

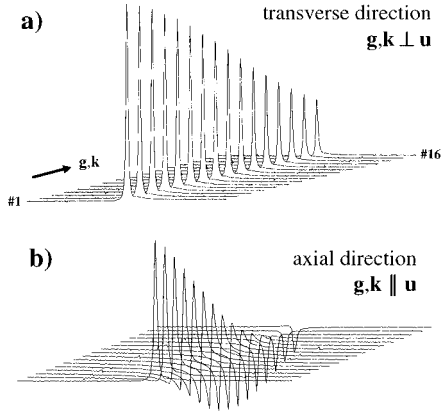

Figure 3. Dependence of the water proton signal (amplitude and phase) on the strength of the applied magnetic field gradient, g and its orientation with respect to the column axis. Measurements made by PFGSE with $\delta = 2$ ms, $\Delta = 40$ ms, on a PEEK column (4.4 mm i.d.) packed with spherical-shaped particles of porous silica ($d_p = 30\ \mu$ m), at a flow rate of 2.2 mL/min. *Figure 3a*: Measurements made in the transverse direction, i.e., perpendicular to the column axis. *Figure 3b*: Measurements made in the direction parallel to the flow direction.

In Figure 3a, the gradient, **g**, hence also $\mathbf{k} = \gamma\delta\mathbf{g}$, is oriented along a direction perpendicular to the column axis. The transverse apparent dispersion coefficient is derived from the second term of the exponent in the RHS of eq 2 ($-k^2 D_{ap}[\Delta - \delta/3]$). The first term of this exponent ($i\mathbf{k}\cdot\mathbf{u}\Delta$) disappears because the field gradient and the mobile phase velocity are oriented in perpendicular direction, so their vectorial product is 0. In this particular experiment, we obtained $D_{ap,t} = 1.28 \times 10^{-4}$ cm^2/s, with a high precision (regression coefficient such that $r^2 = 0.9992$).

In Figure 3b, the measurement of the axial dispersion coefficient was carried out at the same flow rate (2.2 mL/min). **g** and **k** are now oriented parallel to the column axis. Then, two things happen simultaneously. First the amplitude of the water signal decreases with increasing value of the field gradient, because of axial dispersion. This is accounted for by the second term in the exponent of the RHS term of eq 2. From the intensity of this decay, we can derive the axial apparent dispersion coefficient, $D_{ap,a}$. In addition to this effect, there is an increasing phase shift of the recorded signal, illustrated in Figure 3b. This shift is the consequence of the increasing magnitude of the imaginary part of the exponent, which is proportional to the vectorial product, $\mathbf{k}\cdot\mathbf{u}$. This would allow the determination of the mobile phase velocity. Under the experimental conditions of Figure 3b, we find that $D_{ap,a} = 1.49 \times 10^{-3}$, with $r^2 = 0.9996$. Note that, in this case, $D_{ap,a}$ is approximately 1 order of magnitude larger than $D_{ap,t}$.

II. Chromatographic Measurements. a. Instrument. To carry out the PFGNMR measurements, no sample mixture has to be injected into the column. The proton nuclei of the molecules of the mobile phase, here pure water, are directly used as the probes of the flow field and dispersion mechanism. Accordingly, there is no need for a sampling device nor for an on-line detector.

A Bischoff HPLC pump (Bischoff, Leonberg, Germany) was used to pump deionized, degassed water through the column at constant flow rate. It was fitted with a micropump head for low flow rates 0.01 to 0.6 mL/min) and with a regular head for flow rates up to 4.6 mL/min. The flow rates were measured by collecting periodically the mobile phase flowing through the column and weighing it. The pump was located 1.5 m from the magnet. Precolumn filters were placed at the exit of the pump to avoid the introduction of any metallic particle into the column.

To provide an NMR-compatible chromatography setup, the 4.4 mm i.d., 150 mm long columns, the narrow bore connecting tube between

(76) Tanner, J. E. *J. Chem. Phys.* **1970**, *52*, 2523.
(77) Latour, L. L.; Li, L.; Sotak, C. H. *J. Magn. Reson. B* **1993**, *101*, 72.

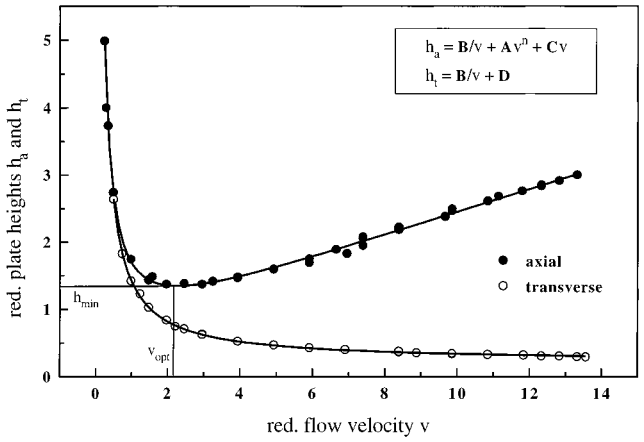

Figure 4. Plots of the axial (h_a) and the transverse (h_t) reduced plate heights vs the reduced flow velocity ($\nu = (ud_p)/D_m$). Column is packed with spherical-shaped particles of monodispersed polystyrene, $d_p = 9$ μm, 40% cross-linked with divinylbenzene. PFGSTE is employed with $\delta = 5$ ms and $\Delta = 69.2$ ms. Mobile phase is H_2O. Parameters obtained from the best fits (solid lines) to the experimental data (symbols), using the equations shown (for $n = 0.33$): $A = 0.36$, $B = 1.19$, $C = 0.16$, $D = 0.22$. $h_{min} = 1.3$, $\nu_{opt} = 2.2$.

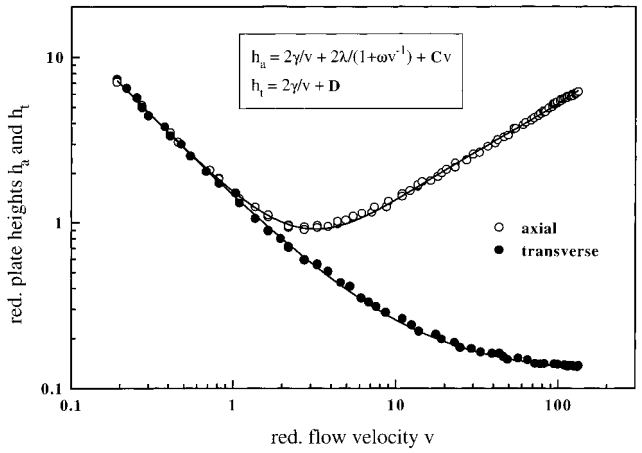

Figure 5. Plots of the axial and transverse reduced plate heights vs the reduced flow velocity. Column is packed with spherical-shaped porous particles of chemically bonded C18 silica ($d_p = 50$ μ m). PFGSE is employed with $\delta = 2$ ms and $\Delta = 22$ ms. Mobile phase is H_2O. Parameters obtained from the best fits (solid lines) to the experimental data (symbols), using the equations shown: $\gamma = 0.67$, $\lambda = 1.46$, $\omega = 20.71$, $C = 0.028$, $D = 0.12$.

the pump and the column, the frits, unions, fingertights, and endfittings were made of PEEK (poly(aryl ether ether ketone)). Most of these parts were manufactured out of a PEEK rod in the workshop of the University of Tübingen. Although PEEK is not a high tensile strength material, inlet pressures up to 250 atm could be used safely with this equipment. This allowed the easy reach of the maximum flow rate that the pump could deliver through the column packed with the silica particles ($d_p = 50$ μm, see later). The polystyrene beads ($d_p = 9$ μm), although heavily cross-linked, could probably not stand a higher pressure without being damaged or partly crushed. Thus, the use of PEEK to manufacture an HPLC chromatograph allows the operation of a chromatographic column of analytical size under realistic conditions.

b. Materials. Using a conventional slurry technique,[55] the columns were packed with one of two packing materials. The first one is made of porous, spherical particles of chemically bonded C-18 silica (fully endcapped), 50 μm in average diameter (YMC Europe, Schermbeck, Germany). The second material is made of spherical particles of monodispersed polystyrene, 9 μm in average diameter, 40% cross-linked with divinylbenzene. 5% slurries of the packing materials were prepared in degassed 2-propanol (silica material) or in deionized, degassed water containing 1% Triton (polystyrene). The packing pressure was 250 atm and the packing was consolidated for 30−40 min under the viscous stress caused by this solvent stream.

Immediately after the silica column was finished packing, its efficiency was determined using the conventional chromatographic procedure, recording chromatograms with a UV−spectrophotometric detector. *N*-Butylbenzene was used as the sample and an 80:20 acetonitrile/water solution as the mobile phase for the C18 silica column.

Results and Discussion

The experimental results are shown in Figures 4−9, as plots of the reduced height equivalent to a theoretical plate ($h = H/d_p$) vs the reduced velocity ($\nu = ud_p/D_m$). In all cases, the symbols represent the experimental results while the lines show the best fit to the models discussed earlier. While the data in Figures 4 and 7 are limited to a reduced velocity lower than 15, those in Figures 5, 6, and 8 extend to a reduced velocity of 140. It becomes clear that data acquired in a narrow velocity range can be fitted by nearly any simple model, while data acquired in a wide velocity range are more discriminating. This explains the inconclusive nature of many early comparison between experimental data and the prediction of the various model HETP equations suggested in the literature.[59] Note also that the best

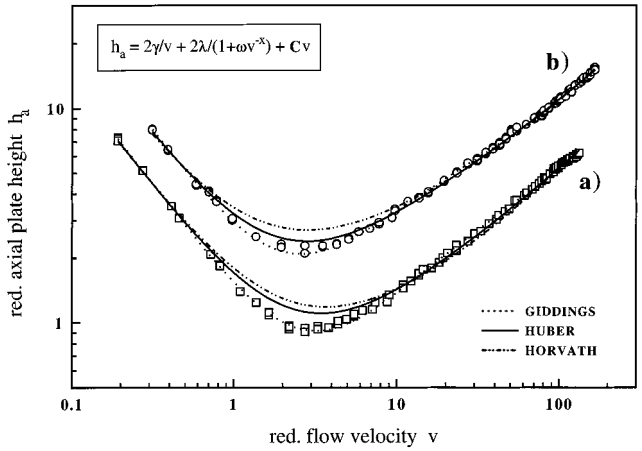

Figure 6. Comparison of the plots of the reduced axial plate height vs the reduced flow velocity obtained (a) from the PFGNMR technique and (b) from conventional chromatographic methods. Column packed was with 50 μm particles of porous C18 silica. The lines shown are the best fits of the experimental data (symbols) to the correlations suggested by Giddings ($x = 1$), Huber ($x = 0.5$), and Horváth and Lin ($x = 0.33$). In either case, the best fit of the data to the Knox equation coincides with that to the Horváth and Lin correlation.

values estimated for the constants of eqs 9 and 10 are close, which explains why these two models are often difficult to rate and compare.

Figure 4 shows the axial and transverse reduced plate heights vs the reduced velocity measured for a column packed with the 9 μm monodispersed polystyrene beads, the mobile phase being pure water. The reduced velocity was derived using the diffusivity of water ($D_m = 1.98 \times 10^{-5}$ cm^2/s at 19 °C). The solid lines are the best fits to the Knox equations for the axial and transverse HETP's. For $n = 0.33$ this gives the following values of the parameters of eqs 10 and 12: $A = 0.36$, $B = 1.19$, $C = 0.16$, and $D = 0.22$. The coordinates of the minimum of the reduced axial plate height curves are $h_{min} = 1.3$ and $\nu_{opt} = 2.2$. The scatter of the experimental data points around the theoretical lines is very small, illustrating the accuracy of these estimates. No systematic deviation of the experimental data from the model can be discerned. However, the range of reduced velocities investigated is limited (0.25−13.5). It was

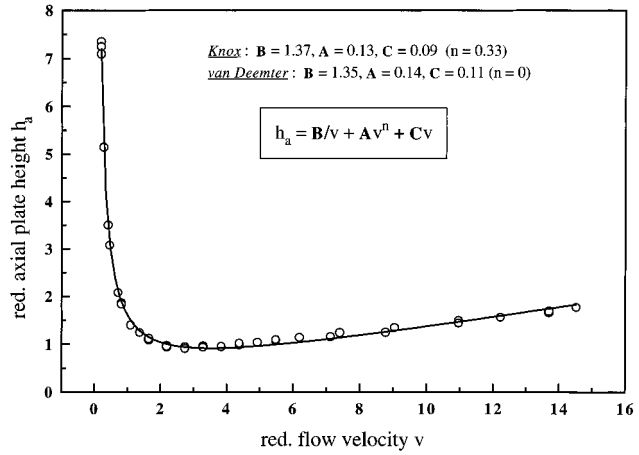

Figure 7. Initial expanded region of the plot of the axial reduced plate height *vs* the reduced velocity shown in Figure 5. Comparison of the experimental data (symbols), and the best fits of these data to the Knox and the van Deemter equations (the two solid lines are overlaid and cannot be distinguished).

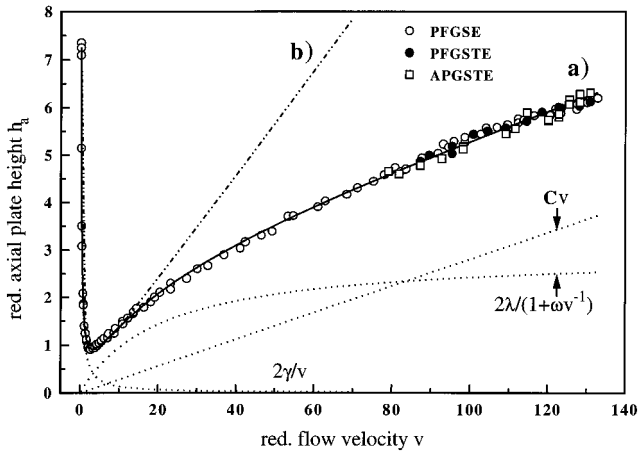

Figure 8. Discussion of the plot of the axial reduced plate height vs the reduced mobile phase velocity. (a) Comparison of the results measured by PFGSE, PFGSTE and APGSTE ($\delta = 2$ ms and $\Delta = 22$ ms) and of these experimental data (symbols) with their best fit to the Giddings equation (solid line). The individual contributions to this equation are represented by the dotted lines. (b) Best fit of the limited set of data shown in Figure 7 to the van Deemter model, extrapolated, with $B = 1.35$, $A = 0.14$, $C = 0.11$ ($n = 0$).

not possible to operate the column under higher inlet pressures and reach a range of reduced velocities (above 30−40) in which the efficiency of the column packed with 50 μm particles do not follow the Knox model any longer.

The values of the axial and transverse reduced plate heights for water in a column packed with the 50 μm C18 porous silica particles are plotted vs the reduced velocity in Figure 5. In this case, a much wider range of reduced velocities, 0.2−140, can be studied because the column is much more permeable. The experimental data points are in excellent agreement with the best fit to the Giddings equations (eqs 6 and 7). There is only a small scatter of the data points around the line and no systematic deviations between the experimental data and the model in any part of the range of reduced velocity investigated. The best estimates of the parameters of the Giddings equations for the axial (eq 6 with $x = 1$) and transverse plate (eq 7) heights thus obtained are $\gamma = 0.67$, $\lambda = 1.46$, $\omega = 20.71$, $C = 0.028$, and $D = 0.12$. The coordinates of the minimum of the curve are $h_{min} = 0.94$ and $u_{opt} = 3.1$. It is worth noting that all the values of h corresponding to ν between 1.95 and 5.4 (curve) or

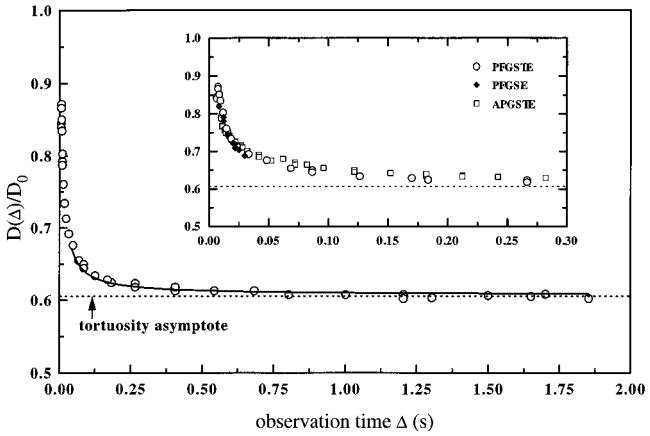

Figure 9. Plot of the normalized diffusion coefficient measured by PFGNMR vs the observation time, Δ, for water, in the column packed with spherical-shaped particles of porous C18 silica ($d_p = 50$ μm). PFGSTE with $\delta = 2$ ms. Molecular diffusivity of water, $D_0 = 1.98 \times 10^{-5}$ cm^2/s, at 19 °C. Experimental data (symbols), best asymptotic fit (solid line), and tortuosity asymptote at $D(\Delta)/D_0 = 0.6$ (dashed line).

between 2 and 5 (experimental results) are below 1. It is useful at this stage to compare the value of this regression and that of a fit of the experimental data to the Knox equation.

Figure 6 compares the best fits of the experimental data (water percolating through a column packed with 50 μm C18 silica particles) to the three fundamental plate height equations, those of Giddings ($x = 1$ in eq 6; dotted line), Huber[13] ($x = 0.5$; solid line), Horváth and Lin[14] ($x = 0.33$; dash−dotted line), and Knox[11] (the best fit to the Knox equation overlay nearly exactly the best fit to the Horváth and Lin equation in the entire range and cannot be distinguished at the scale of the graph). Two sets of experimental results were acquired with the same column and modeled. The first one (a) is the set of efficiency data obtained with the PFGNMR method, as described above. The second set (b) was measured using the conventional approach used in chromatography, on-line detection. In this latter case, *n*-butylbenzene (retention factor, $k' = 3.3$) was chosen as the probe for the efficiency determination, the mobile phase was an acetonitrile/water mixture (80:20), and the HETP was calculated from the width of the peak. These determinations were made immediately after packing the column (i.e., prior to the NMR measurements) and connecting it, with short (and small i.d.) tubes, to a sampling valve with a 10 μL stainless steel loop and to a UV-detector operated at 254 nm. KNO_3 was used for the hold-up time determination. The reduced velocities were calculated from the empirical and approximate Wilke−Chang equation[80] which gives an estimate of the diffusion coefficient of *n*-butylbenzene in the acetonitrile/water mixture used ($D_m = 1.4 \times 10^{-5}$ cm^2 /s). The *n*-butylbenzene band profiles were very symmetrical. The minimum value of the reduced HETP achieved was 2.2 which shows that the column had been very well packed by conventional standards.

The parameters obtained from the best fit of the Giddings equation to the HPLC data are (with the parameters for the PFGNMR data in parentheses) $\gamma = 1.21$ (0.67), $\lambda = 2.62$ (1.46), $\omega = 11.38$ (20.71), $C = 0.062$ (0.028), with $h_{min} = 2.17$ (0.94) for $u_{opt} = 2.7$ (3.1). The correlation was excellent (with $r^2 = 0.999$ in both cases). The difference between the values of the C coefficient is easy to explain. Pure water was used for the PFGNMR measurements and *n*-butylbenzene to record the conventional plate height data. The latter compound is retained on the C18 silica stationary phase and we know that C depends on the retention factor, increasing with increasing k' at low

values of this factor.[55,59−62] The larger value of λ accounts for the markedly higher plate heights (approximately twice larger) observed with the conventional procedure of determination. Note that these measurements were carried out on a freshly prepared column which had not undergone full consolidation, while those reported in ref 47 had been made after completion of the entire investigation, on a consolidated column. Comparing these results with those obtained from determinations of the elution profiles at various locations across the column outlet section[27] suggests that approximately half the band dispersion originates from local sources of dispersion (axial dispersion, *transparticle*, and *transchannel short-range* contributions) while the other half is caused by the nonhomogeneous distribution of the flow velocity (*transchannel long-range*, and *transcolumn contributions*).

Although the correlation given by the Knox equation is less satisfactory than the Giddings equation, the former is so widely used by chromatographers that it is interesting to compare the best estimates of their parameters for the two experimental sets of data in Figure 6. The values of the coefficients of eq 9 for the chromatographic data b are as follows (with the estimates for the PFGNMR data, set a, in parentheses): $b = 2.1$ (1.3), $a = 1.29$ (0.46), $c = 0.05$ (0.031). The correlation coefficient, although smaller than for the fit to the Giddings equation is still satisfactory, with $r^2 = 0.995$ (0.991). It is important to observe that the values of the Knox constants that were derived for our column following the classical efficiency test of an HPLC column are very close to the values that are considered as typical,[55,59−62] while the values derived from PFGNMR are much lower. It has been reported that typical values for well packed columns are $b = 2$, $a = 1$, and $C = 0.01$.[60] The value of C depends very much on the phase system and the probe used. Otherwise, the values of a and b are close to those that we found. Finally, we observe that the model error made by simplifying the eddy dispersion term from the Giddings to the Knox equation leads to significant errors made in the estimate of b and c as well as the eddy dispersion coefficient as well. The classical theory of chromatography assumes that $b = 2\gamma$ and that c is the same in eqs 6 and 9. The values of b and c derived from the Giddings equation, 1.34 and 0.062, respectively, differ significantly from those derived from the same data using the Knox equation, 2.1 and 0.05, respectively.

Figure 7 compares the best fits of the PFGNMR experimental data for the column packed with 50 μm spherical C18 silica particles to the Knox and the van Deemter equations, in a subrange of values of the reduced linear velocity, for ν between 0.2 and 14.5. So, the experimental data are part of those shown in Figure 5. Over this limited range of reduced velocities, the data are fitted equally well by the Knox and the van Deemter equation. The solid lines representing the best fits of both are overlaid. There are only slight differences in the values of the best parameter estimates derived from the two correlations and reported in the figure. Note, however, that the best estimate of c for the Knox equation is quite larger than when the fit of the whole set of data ($0.25 < \nu < 140$) to the Knox equation is done ($c = 0.09$ vs 0.05). The extreme difficulty in distinguishing between the two best curves and sets of parameters explains why it has always been difficult to really distinguish between the two correlations on the basis of experimental data which, even in the best of cases, are not quite as precise as those obtained by PFGNMR.[59] As observed long ago, measurements must be carried out at high values of the reduced velocity in order to observe that the h vs ν plot tapers off.

Figure 8 compares the whole set of data obtained for the axial reduced plate height (derived from the measured dispersion coefficient, symbols), the best fit of these data to the Giddings model (solid line) and to the van Deemter model (dash−dotted line), and the velocity dependence of the different terms of the Giddings model (dotted lines). First, on the experimental front, note the excellent agreement between the data obtained with three different PFGNMR techniques used in this work, PFGSE (pulsed field gradient spin−echo NMR), PFGSTE (pulsed field gradient stimulated echo NMR), and APGSTE (alternating pulsed gradient stimulated echo NMR).

The best values of the parameters obtained from the fit of the data to the van Deemter equation in the range from 0.2 to 14.5 were used to draw the whole curve b in Figure 8. This illustrates how incorrect can be the extrapolation of HETP data acquired at too low values of the reduced velocity. Finally, the three dotted lines in Figure 8 show the variation of each of the three contributions to the reduced HETP in eq 6 with the reduced velocity. The axial diffusion term becomes negligibly small for $\nu > 10$. The eddy dispersion term increases linearly with increasing velocity in that range, then tappers off for $10 < \nu < 40$ and becomes practically constant for $\nu > 50$. The mass-transfer resistance term is smaller than the eddy dispersion term in the whole practical range of operation of HPLC in either analytical or preparative applications. It becomes the largest contribution only for $\nu > 80$. The curves presented in Figure 8 should be compared with those shown by Giddings (ref 8, Figure 2.10-3, p 55) in his discussion of the coupling term contribution, in which he contrasts the coupled and the classical plate height equations.

There are several different techniques available for the determination of dispersion coefficients by PFGNMR. The one described in detail in the Theory section or spin−echo method (PFGSE, open circles in Figure 8) requires, in the approach followed here, the use of gradient amplitudes which decrease with increasing flow rates, i.e., increasing amounts of dispersion (see eq 2), to remain under such experimental conditions that **k** is small (region of initial signal attenuation). There can be limits to the use of low magnetic field amplitudes set by the background gradients which are caused by the magnetic susceptibility contrast between the porous matrix and the water filling the pores of the silica particles. Other PFGNMR techniques are less sensitive to these background gradients in the sample studied. For the sake of comparison, some measurements were carried out at higher flow rates ($\nu > 80$), using two such techniques, PFGSTE and APGSTE. The data obtained are reported in Figure 8. With the APGSTE technique, adapted from Latour et al.,[38,77] these effects should be minimized. The fact that there are no significant differences between the results obtained with these three techniques (Figure 8) is a clear indication that background gradients associated with the water saturated packing used do not constitute a problem in our studies made by PFGNMR at 4.7 T.

Figure 9 illustrates how, by monitoring the observation time in the absence of flow (i.e., the dispersion time), it is possible to investigate the dependence of the molecular diffusivity of water in the packing material under study. This offers a new, direct and simple method of determination of the packing tortuosity. It is sufficient to perform successfully this measurement that the observation time be long enough for the dispersion to approach the asymptotic limit. At very short observation times, the water molecules in a packed bed behave as in a bulk solution. When the observation time, Δ, becomes long, the apparent diffusivity is proportional to the tortuosity of the bed.

In chromatography, the tortuosity of the packing is defined as

$$\gamma = \lim_{\Delta\to\infty} \frac{D(\Delta)}{D_0} \tag{13}$$

At the other extreme, for very short observation times, Δ, the diffusion coefficient $D(\Delta)$ tends toward the molecular diffusivity, D_0. However, it is not possible to achieve extremely small values of Δ. The shortest value of Δ which could be used in our PFGSTE study (Figure 9, open circles) was 8 ms. It was set by the requirement to perform these measurements under conditions satisfying the short gradient pulse limit, $\delta \ll \Delta$ (see Theory, derivation of eq 1). The largest value of Δ used was 1.85 s. It corresponds to an average diffusion length of the water molecules of $l_D = (D_0\Delta)^{1/2} = 60.5$ μm, larger than the average particle diameter.

Equation 13 is the definition of the tortuosity factor in chromatography, γ (with $\gamma = 1/T$, T being the conventional tortuosity of the packing). To relate the apparent dispersion coefficient $D(\Delta)$ (measured in the absence of flow) to the observation time, Δ, Latour et al.[38] have used the following expansion of $D(\Delta)$ in powers of Δ for long observation times[81] where κ_1 and κ_2 are constants that depend on the microscopic

$$\frac{D(\Delta)}{D_0} = \gamma + \frac{\kappa_1}{\Delta} - \frac{\kappa_2}{\Delta^{3/2}} \tag{14}$$

structure of the particle.

The experimental results are shown in Figure 9 (symbols). The best fit of the experimental data to this equation (solid line) gives a tortuosity factor $\gamma = 0.6$. The corresponding asymptote is shown as the dashed line. This method of measurement of γ is very precise and accurate. The inset of Figure 9 shows the same data at a larger scale, illustrating the initial drop of $D(\Delta)/D_0$. The different symbols chosen correspond to the different techniques used to measure the long-time limit of the dispersion coefficient, PFGSTE (open circles) and APGSTE (open squares). The values obtained for the tortuosity factor are 0.6 and 0.62, respectively. This excellent agreement contrasts with the significant and often large differences found with these techniques when using samples of nonporous and porous glass beads or of porous alumina. It demonstrates the superiority of the packing materials used in chromatography over the glass beads and other materials used in previous PFGNMR studies of dispersion in porous materials.[79]

For example, most glass bead materials look unevenly greenish under proper lighting, showing them to contain large amounts of iron. This paramagnetic impurity seriously perturbs the local magnetic field. Furthermore, these materials have a very wide size distribution which makes difficult the preparation of an homogeneous bed. By contrast, the concentration of most samples of chromatographic silica in paramagnetic ions is very low. When on the surface of the adsorbent, these ions would give strong Lewis acid adsorption sites which adversely affect the chromatographic performance. The only practical method to reduce the surface concentration of these ions is to reduce their bulk concentration. Silica for chromatography is usually prepared by hydrolysis of very pure solutions of ethyl silicate, hence the low metal concentration of the packing materials. Particularly, the iron concentration of the YMC material used here is nominally below 10 ppm and is in many lots of the order of a few parts per million. This is a much lower concentration than the one found in many sands, glass beads, and other pulverulent materials often used in NMR studies of dispersion. Also, the particle size distribution in these materials is narrow, which allows the preparation of relatively homogeneous consolidated beds of the material.

A comparison similar to the one described in Figure 9 for the column packed with the water-saturated spherical-shaped 50 μm porous silica particles (YMC material) was performed for the column packed with the 9 μm monodispersed polystyrene particles (data not shown). The value found for the tortuosity factor, γ, was 0.59. This value compares well with the tortuosity factor obtained for silica by PFGNMR under static conditions (0.60 and 0.62) and by the analysis of the van Deemter plots, i.e., under flow conditions of the polystyrene packing: $b = 2$, $\gamma = 1.19$. These values of the tortuosity of the two columns are consistent with the conventional assumption that the tortuosity coefficient, $\gamma = 1/T$ (T, conventional tortuosity), is close to the square root of the external porosity.[82,83] This assumption leads to the reasonable estimates of external porosities of 0.36 to 0.38 for the 50 μm silica particle column and of 0.35 for the 9 μm particle polystyrene column. These estimates are in excellent agreement with those derived for similar materials using entirely different approaches (inverse size exclusion chromatography, mercury porosimetry, and chromatographic determinations).[22]

The larger value of γ derived from the PFGNMR measurements of the axial dispersion coefficient at different flow velocities in the case of the 50 μm silica packing (0.67, to be compared to 0.6 and 0.62 obtained from the tortuosity asymptote, Figure 9) is probably explained by the low value of the observation time used in these measurements ($\Delta = 22$ ms). As confirmed by the results shown in Figure 9, the full tortuosity of the packing is still not completely felt by the fluid molecules in the region of low Peclet numbers. It is indeed approximately 0.70 at $\Delta = 22$ ms. This difference is not very large. For the much smaller polystyrene particles, $\Delta = 69.2$ ms, and the two estimates of the tortuosity are nearly identical under these conditions.

The combination of PFGNMR and NMR imaging methods allows the mapping of the axial or radial dispersion coefficients in a thin slice across the column. By performing systematically such measurements, in series of slices of appropriate location and orientation, it is possible to determine the detailed anatomy of the dynamics of chromatographic columns. Finally, PFGNMR methods allow the investigation of the mass-transfer kinetics between the mobile phase percolating through the particles and the solvent contained inside the particle pores. This is achieved by using the propagator formalism in a way allowing the quantitative characterization of the spectrum of the net displacements of the fluid molecules at different observation times and flow rates. The results obtained in these different investigations will be reported separately.

Acknowledgment. This work has been supported in part by Grant DE-FG05-88ER13859 of the U.S. Department of Energy and by the cooperative agreement between the University of Tennessee and the Oak Ridge National Laboratory. We thank Ulrich Trüdinger (YMC Europe, Schermbeck, Germany) for the generous gift of the packing material and Hans Fritz (Institute of Organic Chemistry, University of Tübingen, Germany) for providing us with the monodispersed polystyrene particles.

JA9726623

(78) Koh, J.-H.; Guiochon, G. *J. Chromatogr. A* In press.
(79) Tallarek, U.; Bayer, E.; Guiochon, G. Unpublished results.
(80) Wilke, C. R.; Chang, P. *AIChE J.* **1955**, *1*, 264.
(81) Haus, J. W.; Kehr, K. W. *Phys. Rep.* **1987**, *150*, 263.
(82) Wong, P.-Z.; Koplik, J.; Tomanic, J. P. *Phys. Rev. B* **1984**, *30*, 6606.
(83) Roberts, J. N.; and Schwartz, L. M. *Phys. Rev. B* **1985**, *31*, 5990.